Journal of Petroleum Science and Engineering 213 (2022) 110388

Contents lists available at ScienceDirect

Journal of Petroleum Science and Engineering

journal homepage: www.elsevier.com/locate/petrol

Magnetically inferred regional heat flow and geological structures in parts of Chad Basin, Nigeria and their implications for geothermal and hydrocarbon prospects

Musa O. Awoyemi [a], Sesan C. Falade [b,c,*], Augustine B. Arogundade [a], Olaide S. Hammed [d], Ojudoo D. Ajama [e], Ayomiposi H. Falade [f], Leke S. Adebiyi [b,c], Kehinde O. Dopamu [b,c], Esther A. Alejolowo [c]

[a] Department of Physics and Engineering Physics, Obafemi Awolowo University, Ile-Ife, Nigeria
[b] Landmark University SDG 7 (Affordable and Clean Energy Research Group), Nigeria
[c] Department of Physical Sciences, Landmark University, Omu-aran, Nigeria
[d] Department of Physics, Federal University, Oye-Ekiti, Nigeria
[e] Ondo State Ministry of Education, Science and Technology, Akure, Nigeria
[f] Department of Geology, Obafemi Awolowo University, Ile-Ife, Nigeria

ARTICLE INFO

Keywords:
Geothermal energy
Hydrocarbon
Curie point depth
Aeromagnetic
Chad Basin

ABSTRACT

This study analysed high-resolution aeromagnetic data over part of Chad Basin, Nigeria to determine the implications of geological structures and heat flow on the geothermal and hydrocarbon potential of the basin. Curie Point Depth (CPD) analysis, Curvature analysis and Source Parameter Imaging (SPI) were applied in this study. The estimated CPD and heat flow range from 11 to 19 km and from 75 to 125 mW/m^2 respectively. The geological structures in the area predominantly trend in the E-W direction, followed by the ENE-WSW direction. Other prominent structural trends include NE-SW and WNW-ESE. The depths to the magnetic sources range from about 0.1 km to over 5 km. A large number of shallow-seated magnetic structures, believed to be intra-sedimentary intrusive bodies, were mapped in the southern and northwestern parts of the study area. The estimated heat flow in Chungul Buturi and Gumsa areas was found to be sufficient for the economic exploitation of geothermal energy. The results of this study showed that the basin is thermally matured for hydrocarbon generation. However, high magnitudes of heat flow and the presence of a large number of intrusive bodies in parts of the basin might have been the reason behind the unsuccessful attempts to find hydrocarbon in commercial quantities in the basin. The results also showed that the basin has a higher potential for gas accumulation than oil. Future exploration for commercial hydrocarbon accumulation in the basin may be successful if the exploration sites are narrowed down to the regions where moderate heat flow, high sedimentary thicknesses with few shallow seated magnetic sources (intrusives), and elongated geological structures were mapped in this study.

1. Introduction

The magnetic signature of the crust is observed as anomalies in the magnetic field of the Earth. These anomalies are exploited in the magnetic method of geophysics to investigate the Earth's subsurface. The magnetic method is used as a tool for locating mineral deposits, studying basin structure and its hydrocarbon potential, mapping geological features, and identifying geothermal resources, among others (Nabighian et al., 2005). In the search for geothermal energy and hydrocarbon fluids, the magnetic method involving the use of high-resolution aeromagnetic data (HRAD) helps in determining the geothermal and hydrocarbon potential of a basin by providing reconnaissance information on the geological structures, and as well as the thermal structure, of the Earth's crust.

The global call for clean and renewable energy to ensure a healthy energy-nature loop has necessitated the regional-scale search for alternatives to fuel-fired energy production. The increasing energy demands of human beings and the carbon-induced climate irregularities direct

* Corresponding author. Landmark University SDG 7 (Affordable and Clean Energy Research Group), Nigeria. ,
E-mail addresses: faladesesan@gmail.com, falade.sesan@lmu.edu.ng (S.C. Falade).

https://doi.org/10.1016/j.petrol.2022.110388
Received 31 December 2021; Received in revised form 23 February 2022; Accepted 8 March 2022
Available online 10 March 2022
0920-4105/© 2022 Elsevier B.V. All rights reserved.

energy demands towards geothermal energy, which is a natural energy of the Earth. A carbon-free energy future could be achieved through the exploitation of geothermal energy. However, identifying the suitable region for geothermal exploitation requires information about the thermal structure of the crust. Several studies have attempted to estimate the thermal structure of the Chad Basin Nigeria from near-surface heat-flow measurements. Nwankwo et al. (2009) estimated a heat flow range of 63.6–105.6 mW/m^2 from well log data acquired from 14 oil wells. Nwankwo and Ekine (2009) estimated the thermal gradients to be within the range of 30–44 °C/km with a mean value of 34 °C/km using temperature data from 21 oil wells. Also, Kwaya et al. (2016), using oil and water well data, estimated thermal gradient values ranging from 28.1 to 58.8 °C/km, with a mean value of 37.1 °C/km. Near-surface geothermal measurements, which have been the conventional method for estimating the crustal thermal structure, suffer some setbacks as they may be contaminated by local thermal anomalies; are rarely distributed geographically evenly; and are usually insufficient to define regional geothermal structures (Tanaka et al., 1999; Ross et al., 2006). Several studies have shown good correlations between the known thermal structures and those estimated from the depth to the bottom of magnetic sources (DBMS) which were determined from spectral analysis of aeromagnetic data (e.g. Tanaka et al., 1999; Ross et al., 2006; Okubo et al., 1985; Okubo and Matsunaga, 1994; Li et al., 2017). The DBMS, although may represent petrological/compositional boundary, is used synonymously with Curie point depth (CPD) due to the non-magnetic behaviour of the crust below the CPD. The CPD is the depth at which magnetic minerals in rocks attain their Curie temperature. Below the CPD, the rocks are non-magnetic due to increasing temperature. The CPD helps in understanding the crustal thermal structure under the assumption of vertical temperature gradient in the lithosphere. The thermal structure can be used to evaluate the geothermal resource and hydrocarbon potentials of a sedimentary basin. In this study, the CPD is assumed to be the depth to the deepest level in the crust containing minerals that produce anomalies in the magnetic field of the Earth.

Interest in sedimentary basins arises from the fact that they are usually potential hosts for oil, gas, minerals, and groundwater. It has been established that the Chad Basin in Nigeria has some favourable critical criteria for high hydrocarbon prospect (Reyment, 1965; Matheis and Kogbe, 1976; Agagu and Ekweozor, 1980; Petters, 1981; Avbovbo et al., 1986; Okosun, 1995; Palumbo et al., 1999; Obaje et al., 1999; Adekoya et al., 2014). Also, significant oil discoveries in commercial quantities have been made in neighbouring basins, such as Termit Basin in the Niger Republic and Doba Basin in the Chad Republic, whose source rocks and rift system are similar to those observed in the Nigerian sector of the Chad basin (Obaje et al., 2004; Mijinyawa et al., 2013; Aderoju et al., 2016). However, efforts made by the Nigerian Government through the Nigerian National Petroleum Corporation (NNPC) to find commercial oil and gas accumulation in the basin have not been successful despite intensive 2D and 3D seismic surveys and drillings (Obaje et al., 2004; Aderoju et al., 2016; Nwankwo et al., 2012). Most wells acquired by the NNPC were dry, with a few having some gas or oil shows with no evidence of commercial quantity (Aderoju et al., 2016). There is therefore the need to interpret the available geophysical data that can help to suggest, at a regional scale, the possible cause of many dry wells in the basin and areas that are favourable for successful hydrocarbon exploration in the basin. Hence, this study aimed at analysing and interpreting the HRAD over the area to provide reconnaissance information that will serve as a guide in the ongoing prospecting for hydrocarbon in the area, as well as, in assessing the geothermal potential of the basin.

2. Geology and tectonic settings of Chad Basin Nigeria

The Chad Basin is an inland basin that was created when Gondwana split and the South American and African plates were separated (Aderoju et al., 2016). The basin straddles into Chad Republic, Nigeria, Cameroon, Niger and the Central African Republic, with Chad and Niger sharing more than a half of it (Obaje, 2009). The Nigeria's portion of the Chad Basin (locally referred to as Bornu Basin) is situated in the north-eastern region of the country and covers nearly a tenth of the entire Chad Basin. Fig. 1 shows the Chad Basin Nigeria as one of the major geological units in the country. The basin's epochs of sedimentation range from Albian to Quaternary (Avbovbo et al., 1986) and the majority of the sediments were deposited during the Cretaceous period. The basin consists of six stratigraphic units (see Fig. 2), namely, the Bima Sandstone at the bottom, followed by the Gongila Formation, Fika Shale, Gombe sandstone, Kerri–Kerri Formation and Chad Formation. The oldest stratum (Bima Sandstone) is from Albian to Cenomanian ages. It comprises continental, fossiliferous, thin to thick beds of coarse to fine-grained, feldspathic sandstones, which lie unconformably on the Pre-Cambrian basement (Avbovbo et al., 1986; Okosun, 1995). It also includes thin shales and intercalations of sandstone with a thin band of clay and siltstone (Okosun, 1995; Ahmed et al., 2022). The earliest deposition of marine sediments in the basin occurred during the Turonian age. The Gongila Formation rests conformably on the Bima Sandstone. It represents a transition from continental to marine sediments. It consists of interbedded shale, sandstone, layers of volcanic intrusive bodies occurring as diorite sills, and fossilized and non-fossilized limestone (Okosun, 1995; Ahmed et al., 2022). The Fika Shale consists of Turonian to Santonian marine sediments, which are mainly locally gypsiferous marine blue-black shale with thin limestone intercalations. Volcanic intrusive, which occurred as diorite sills, are emplaced at several horizons in the Fika Shale. The Gombe Sandstone is present only in some parts of the Chad Basin. It is a deltaic/lacustrine sedimentary formation that occurred during the Maastrichtian. It consists of interbedded sandstone, shale, siltstone, and clay. The Gombe Sandstone is overlain by the continental deposits (Kerri-Kerri Formation) of Paleocene age. The Kerri-Kerri Formation comprises thin and thick beds of grit, sandstone and gritty clay. The Chad Formation, which is the youngest stratigraphic unit in the basin, is made up of continental (lacustrine) and Quaternary sediments consisting of sandy strata interlayered by clay. The petroleum source rocks in the basin are believed to exist within the Fika Shale and Gongila Formation (Moumouni, 2009).

Tectonically, the framework and evolution of the basin are characterized by four stages: Pan African Crustal Consolidation (750–550 Ma), Early Rift (130–98 Ma), Late Rift (98–75 Ma) and Post Rift stages (66–0 Ma). Major basement structures, including the NE–SW trending fault system of the basin, were created during the Pan African crustal consolidation (Obaje, 2009). The rift system that resulted in the creation of the basin occurred during the Early Rift stage. The tectonic activities of the Late Rift produced geological structures that include NW-SE trending faults and folds. The majority of the faults in the basin resulted from movements along the basement faults (Okosun, 1995). The basin's significant tectonic events ended before the Post Rift stage. Hence, the Tertiary and Quaternary strata have no notable faulting or significant folding.

3. Materials and methods

The HRAD sheets covering Latitudes $11°00' - 13°00'$N and Longitudes $11°30' - 14°00'$E in the Chad Basin Nigeria were used. The data are parts of the nationwide HRAD acquired in 2006 and 2007 by Fugro Airborne Surveys (FAS). The aeromagnetic surveys were carried out on behalf of the Nigerian Geological Survey Agency (NGSA). The magnetic sensor was flown at a nominal altitude of 80 m, and data were collected every 0.1 s along a set of NW-SE flight lines, spaced 500 m, with a tie-line spacing of 2000 m in the NE-SW direction. All necessary data corrections, including the International Geomagnetic Reference Field (IGRF) removal, were performed by FAS.

The HRAD is presented as Total Magnetic Intensity (TMI) anomaly map in Fig. 3a. The study area is in low geomagnetic latitudes (i.e.,

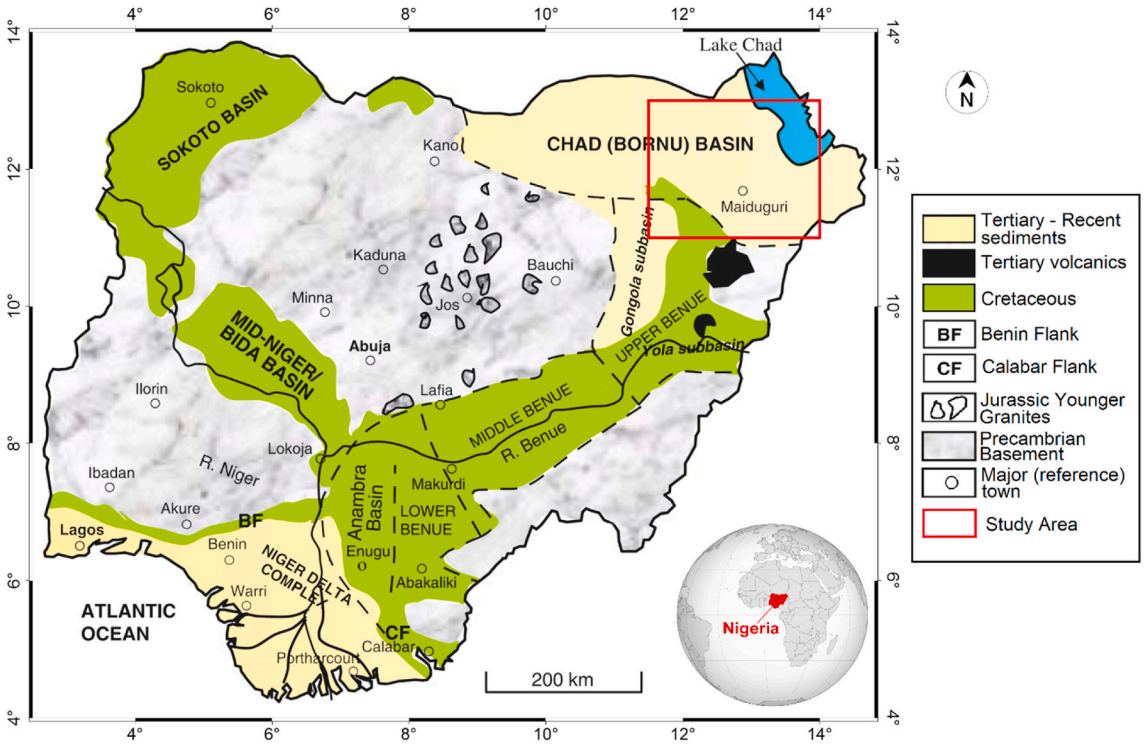

Fig. 1. The Nigerian Geological Map showing the study area within the Chad (Bornu) Basin (Adapted from Obaje et al., 2006).

latitudes with magnetic inclinations of less than 15°) where the reduction of data to the geomagnetic pole is generally unstable. The effect of the geomagnetic inclination on the study area was, therefore, corrected by reducing the TMI anomaly map to the equator. The reduced to equator (RTE) anomaly map (Fig. 3b) produced is an enhanced TMI anomaly map in which the anomalies are centred over their causative bodies, thereby, making the anomaly interpretation easier and more accurate.

3.1. Determination of CPD and heat flow

The well-established centroid approach to CPD estimation (Tanaka et al., 1999; Okubo et al., 1985; Bansal et al., 2011) was used in this study. The centroid method, which is the most currently used method (Quintero et al., 2019), gives more reliable depth estimates compared to other CPD estimation methods such as forward modelling and spectral peak method (Ravat et al., 2007). The centroid method computes the CPD (Z_b) using the relation (Okubo et al., 1985):

$$Z_b = 2Z_c - Z_t \tag{1}$$

where Z_c and Z_t are the centroid and top depths of the deepest magnetic body. The values of Z_t and Z_c are estimated from the power spectral density ($P(k)$) of magnetic data using the relations (Bansal et al., 2011):

$$\ln\left(k^{\beta}\, P(k)\right) = A_1 - 2|k|Z_t \tag{2}$$

and

$$\ln\left(k^{\beta}\frac{P(k)}{k^2}\right) = A_2 - 2|k|Z_c \tag{3}$$

respectively; where k is the wavenumber, A_1 and A_2 are constants, and β is a scaling exponent used to correct the spectrum to allow for fractal distribution of sources (Bansal et al., 2011, 2013). The value of β depends on the lithology and heterogeneity of the subsurface. The conventional centroid method (Tanaka et al., 1999; Okubo et al., 1985) assumes that the source distribution is random and uncorrelated, while the Modified Centroid Method of (Bansal et al., 2011, 2013) assumes that the distribution of sources is fractal, i.e. random and correlated, in nature. These two centroid methods were considered in this study. If β is taken to be zero in Equations (2) and (3), the equations are applicable to the conventional centroid method. However, if $\beta > 0$, the equations are for the Modified Centroid Method. Using the Modified Centroid Method, the value of β must be chosen carefully, since the estimation of the scaling exponent from inversion method produces unrealistic values (Bansal et al., 2013). Using high value of β must also be avoided because it may lead to overcorrection of the spectrum. According to Ravat et al. (2007), estimating depths by correcting the power spectrum with the scaling exponent set to a fixed value of 3 overcorrects the power spectrum. Bansal et al. (2011) suggested that the value of β must be ≤ 2 otherwise the spectrum will be overcorrected, while Bansal et al. (2013) stated that a value of $\beta > 1.5$ also results in overcorrection. Quintero et al. (2019) and Bansal et al. (2013) considered $\beta = 1$ for correcting the power spectrum. This value (i.e. $\beta = 1$) was tried for the study area, and at posteriori, it was appropriate. With this value, the low wavenumber segments of the power spectrum from which depth information was obtained were well defined and the estimated depths were realistic when compared with estimations from oil well data.

CPD provides a proxy for calculating temperature-at-depth, and invariably the heat flow through the crust. The geothermal gradient and heat flow were estimated under the assumptions that there is constant vertical temperature gradient and the layer between the surface and the CPD has no heat sources/sinks (Tanaka et al., 1999). Following this assumption, the geothermal gradient is the ratio of the difference between the Curie temperature and surface temperature to the CPD (relative to the surface). The heat flow is given by:

$$Q = k\left(\frac{dT}{dZ}\right) = k\left(\frac{\theta_c - \theta_s}{z_b}\right) \tag{4}$$

Where (dT/dz) is the geothermal gradient, θ_c is the Curie temperature, θ_s is the surface temperature and k is thermal conductivity. The annual mean surface temperature of the Chad Basin Nigeria is $28^{\circ}C$ (Tyoh et al., 2021). Studies have shown that the Curie temperature of the dominant

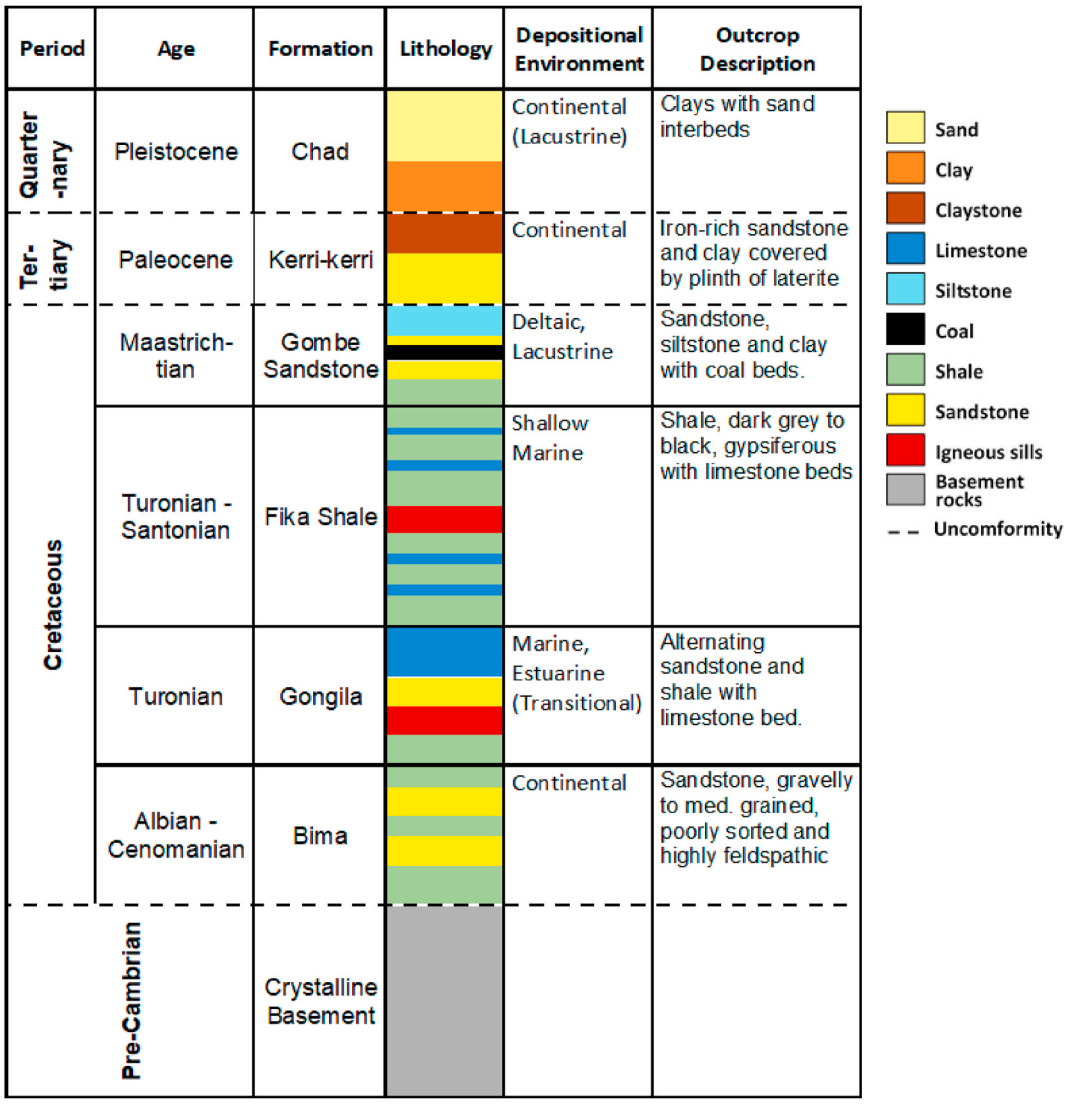

Fig. 2. Generalized lithostratigraphy of the Chad Basin Nigeria (After (Avbovbo et al., 1986; Adegoke et al., 2015)).

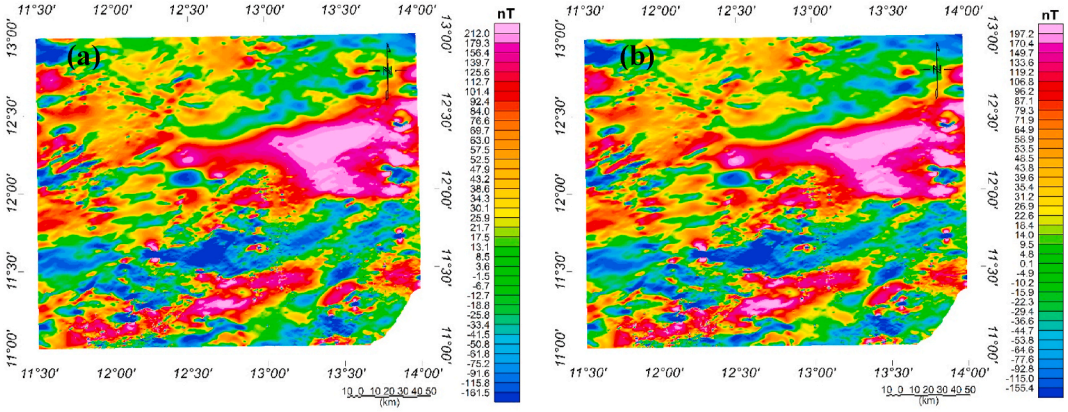

Fig. 3. (a) TMI anomaly map and (b) RTE anomaly map.

mineral in deep continental crustal rocks that produces magnetic anomalies of long-wavelength is about 580°*C* (Frost and Shive, 1986; Stacey, 1977), hence, thermal gradients were computed from the CPD using Curie temperature value of 580°*C*. The average thermal conductivity for igneous rocks is 2.5 $Wm^{-1}C^{-1}$ (Stacey, 1977). For the sedimentary section, the average thermal conductivity value of the major formations of the Nigerian Chad Basin is assumed. According to Dieokuma et al. (2013), the average thermal conductivity values of the Bima, Gongila, Fika and Chad formations are 2.879 $Wm^{-1}C^{-1}$, 2.470 $Wm^{-1}C^{-1}$, 2.432 $Wm^{-1}C^{-1}$ and 2.397 $Wm^{-1}C^{-1}$ respectively. This

implies that the average thermal conductivity of the Basin is $\sim$ 2.5 $Wm^{-1}C^{-1}$, which is similar to that of the basement rock. Hence, heat flow values were computed using $k = 2.5\ Wm^{-1}C^{-1}$.

The study area has a dimension of about 275 km × 220 km. The average CPD of the study area was estimated from the power spectra of the entire RTE anomaly data using the conventional centroid method (Fig. 4a) and the modified centroid method (Fig. 4b). The CPD values were first computed relative to the data elevation (RDE) and then, relative to the ground level (RGL).

In order to obtain more CPD samples that could show the variation of CPD across the study area, the RTE anomaly data was subdivided into twelve parts with 110 km × 110 km 50% overlapping blocks (Fig. 5a). Larger window sizes were avoided considering the limited size of the study area and the fact that they could include contributions of different geological and tectonic environments (Bansal et al., 2011, 2013; Quintero et al., 2019; Ravat et al., 2007). Prior to the subdivision, the data were upward continued to 2 km to suppress the effects of near-surface and intra-sedimentary sources. Filtering for removal of the regional field was avoided for the reason that it may alter the low wavenumber portion of the power spectra and as well, the CPD estimates (Ravat et al., 2007). The IGRF (Degree 13) model used for the compilation of the dataset is enough for separating the crustal field from the geomagnetic field (Ravat et al., 2007). The power spectral densities of the blocks were computed in the Fourier domain. The power spectra and the respective CPD estimates for two blocks (blocks 9 and 10) are presented as examples in Fig. 5b for the conventional centroid method and Fig. 5c for the modified centroid method. The presented spectra are just up to a wavenumber of 2.5 rad/km. The estimated CPDs, computed relative to the earth surface, for all block locations are shown in Fig. 6.

Different authors (e.g. Nwankwo and Ekine, 2009; Kwaya et al., 2016; Shirputda, 2019) have estimated different but close values of the geothermal gradient of Chad basin Nigeria from corrected Bottom Hole Temperature (BHT) data collected from oil exploration wells. The reports by the authors are summarised in Table 1.

In this study, the geothermal gradients derived from the estimated CPD values based on the conventional centroid method and modified centroid method are shown in Fig. 7a and b respectively. The average value of the geothermal gradients for each oil well in Table 1 is indicated on the maps (Fig. 7a and b) to determine the centroid method whose estimates are closer to the values obtained from the oil wells. As shown in Fig. 7, the modified centroid method produced closer geothermal gradient values and was therefore considered more reliable and used to produce CPD and heat flow maps of the study area.

3.2. Mapping of geological structures

Geological structures were automatically interpreted from the RTE anomaly data using curvature analysis (Phillips et al., 2007). The algorithm automatically extracts maxima with strike directions from a special function grid of potential field data whose maxima directly coincides with the locations of source edges. The special function used in this study was the 3D Analytic Signal Amplitude (ASA) (MacLeod et al., 1993). The ASA was applied to the RTE anomaly data at different upward continuation heights (100 m, 1 km, 3 km and 5 km) to map structural features ranging from shallow to deep depths. The upward continuation enhances the effect of deep-seated magnetic sources. The higher the upward continuation height, the more the geological structures at deep depths are revealed, and the more the effects of geological structures at shallow depths are suppressed. Integrating the lineaments of geological structures inferred at various upward continuation heights (in increasing order) reveals the continuity of the geological structures with depth and helps in differentiating the structures that are limited to shallow depths from those that extend to deep depths or are deep-seated. Fig. 8 shows the analytic signal maps corresponding to the upward continuation heights of 100 m, 1 km, 3 km and 5 km. The black lines on the maps indicate the lineament extracted from the ridges (linear set of maxima) of the analytic signal grids. The extracted lineaments were integrated to form a composite map that depicts the geological structures in the study area and the continuity of the structures with depth.

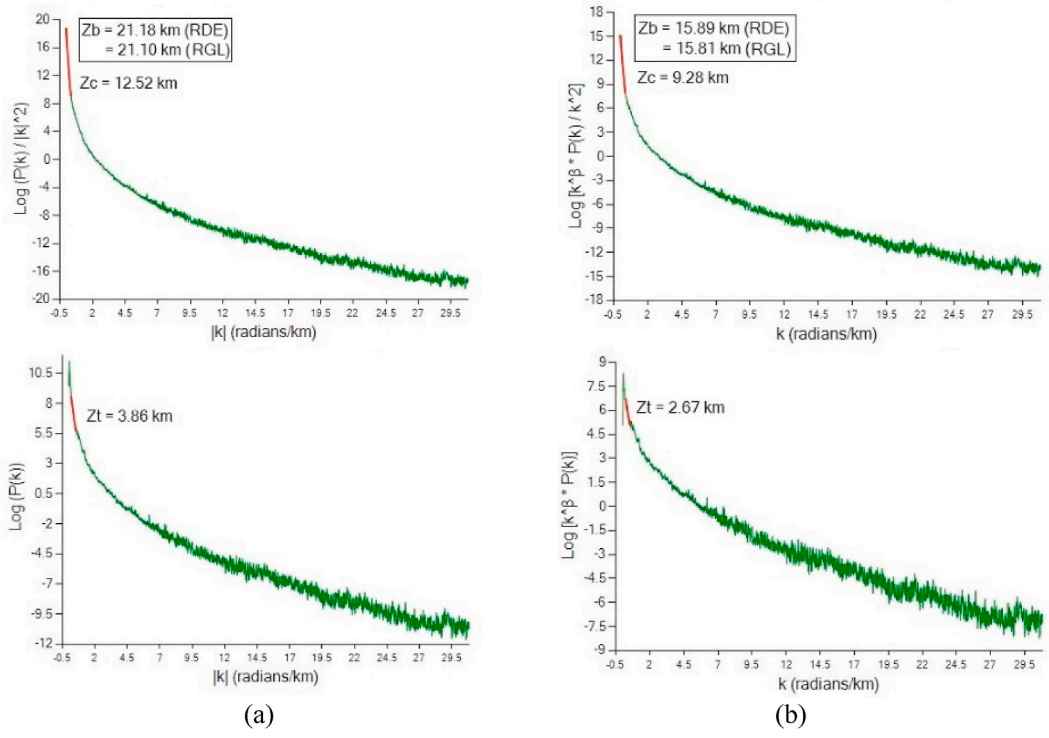

Fig. 4. Estimation of CPD from the power spectra of the entire study area based on (a) the conventional centroid method and (b) the modified centroid method.

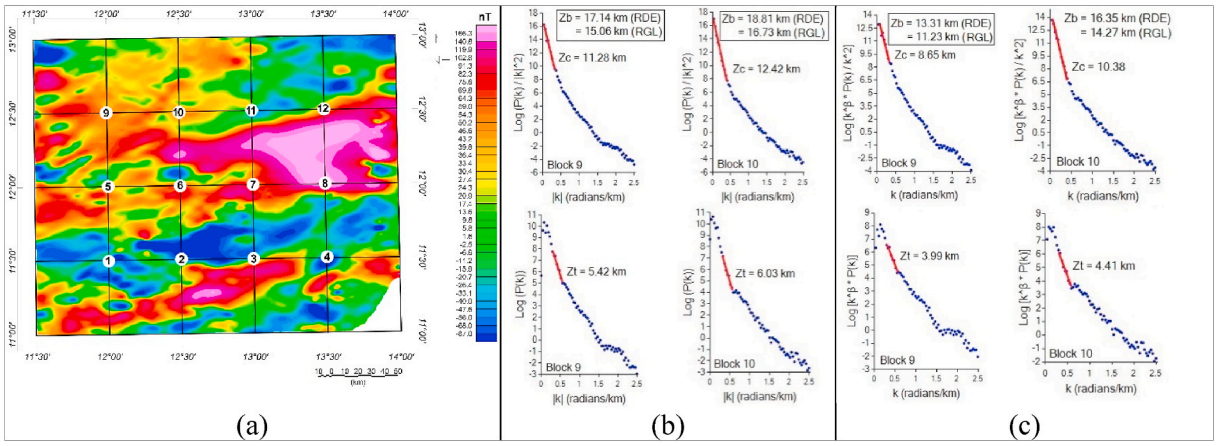

Fig. 5. (a) Filtered RTE anomaly map with the centres of the twelve overlapping blocks labelled on it. The examples of spectra and the respective CPD (Zb) estimation for block 9 and block 10 based on (b) the conventional centroid method and (c) the modified centroid method. The lower and upper portions indicate the top depth (Zt) and centroid depth (Zc) respectively.

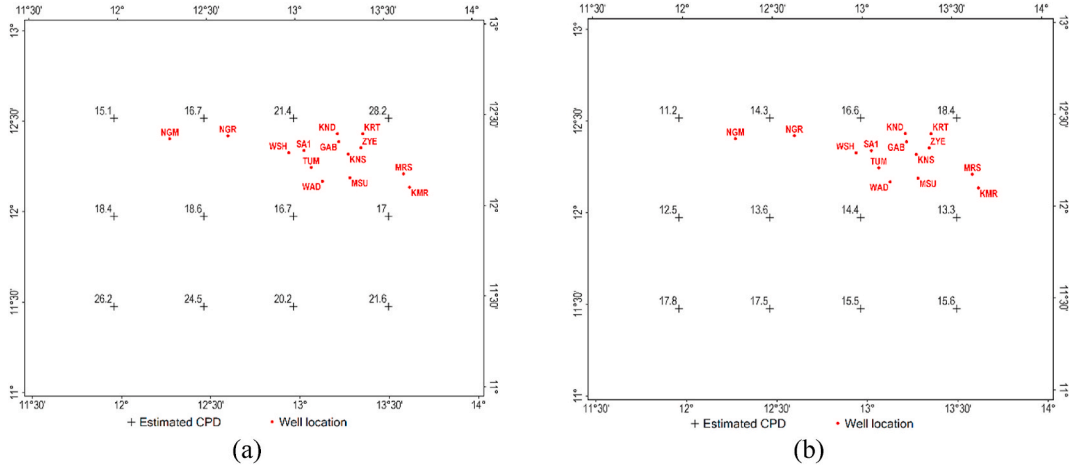

Fig. 6. The estimated CPDs (relative to the ground surface) for all blocks based on (a) the conventional centroid method and (b) the modified centroid method. The CPD values are in km. The names and locations of the known oil wells in the study area are shown in red colour. (For interpretation of the references to colour in this figure legend, the reader is referred to the Web version of this article.)

Table 1
Geothermal gradients in °C/km obtained in recent studies from BHT data collected from oil wells.

Well ID	Well	Nwankwo and Ekine (2009)	Kwaya et al. (2016)	Shirputda (2019)	Average
GAB	GAIBU-1	–	–	41	41
KND	KANADI-1	38	50.2	36	41.4
KMR	KEMAR-01	37	58.8	42	45.9
KNS	KINASAR-01	36	36.1	41	37.7
KRT	KRUMTA_1	34	30.8	34	32.9
MSU	MASU-1	35	36.7	36	35.9
MRS	MURSHE-01	30	29.9	33	31
NGM	NGAMMAEAST-1	36	42.9	40	39.6
NGR	NGORNORTH-1	31	–	34	32.5
SA1	SA-1	33	47.1	55	45
TUM	TUMA-01	34	31.4	39	34.8
WAD	WADI-1	32	37.4	41	36.8
WSH	WUSHE-1	–	33.4	36	34.7
ZYE	Ziye-1	30	32.8	33	31.9

3.3. Estimation of depths to magnetic sources

The depths of magnetic sources in the area of study were estimated from the TMI anomaly data using Source Parameter Imaging (SPI) technique. The technique, developed by Thurston and Smith (1997), computes depths rapidly from the inverse of the peaks of the local wavenumber of the magnetic data without depending on magnetic parameters such as inclination, declination and remanent magnetization, and geological parameters such as the strike and dip of the structures. The TMI anomaly data was upward continued to 100 m before the derivatives used for SPI depth estimations were computed. This was done to suppress the effects of possible near-surface non-geologic (cultural) sources in data. The SPI depth solutions were gridded and presented relative to the ground level as a magnetic source depth map.

4. Results and discussion

Fig. 3 reveals the magnetic anomalies of the study area. The anomaly values range from about −162 nT to 212 nT on the TMI map, and from about −155 nT to about 197 nT after reduction to the equator. The RTE anomaly map shows magnetic anomalies that are more centred over the causative bodies. The variation in the intensities of the anomalies is due to the differences in the susceptibilities, geological boundaries and

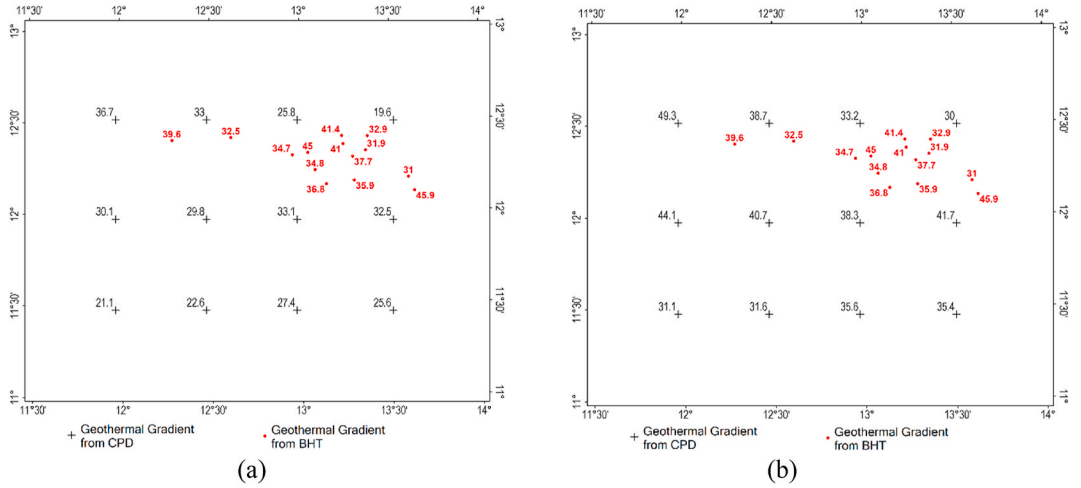

Fig. 7. The estimated geothermal gradients (in °C/km) for all blocks based on (a) the conventional centroid method and (b) the modified centroid method. The geothermal gradient values obtained from oil wells in the study area are shown in red colour. (For interpretation of the references to colour in this figure legend, the reader is referred to the Web version of this article.)

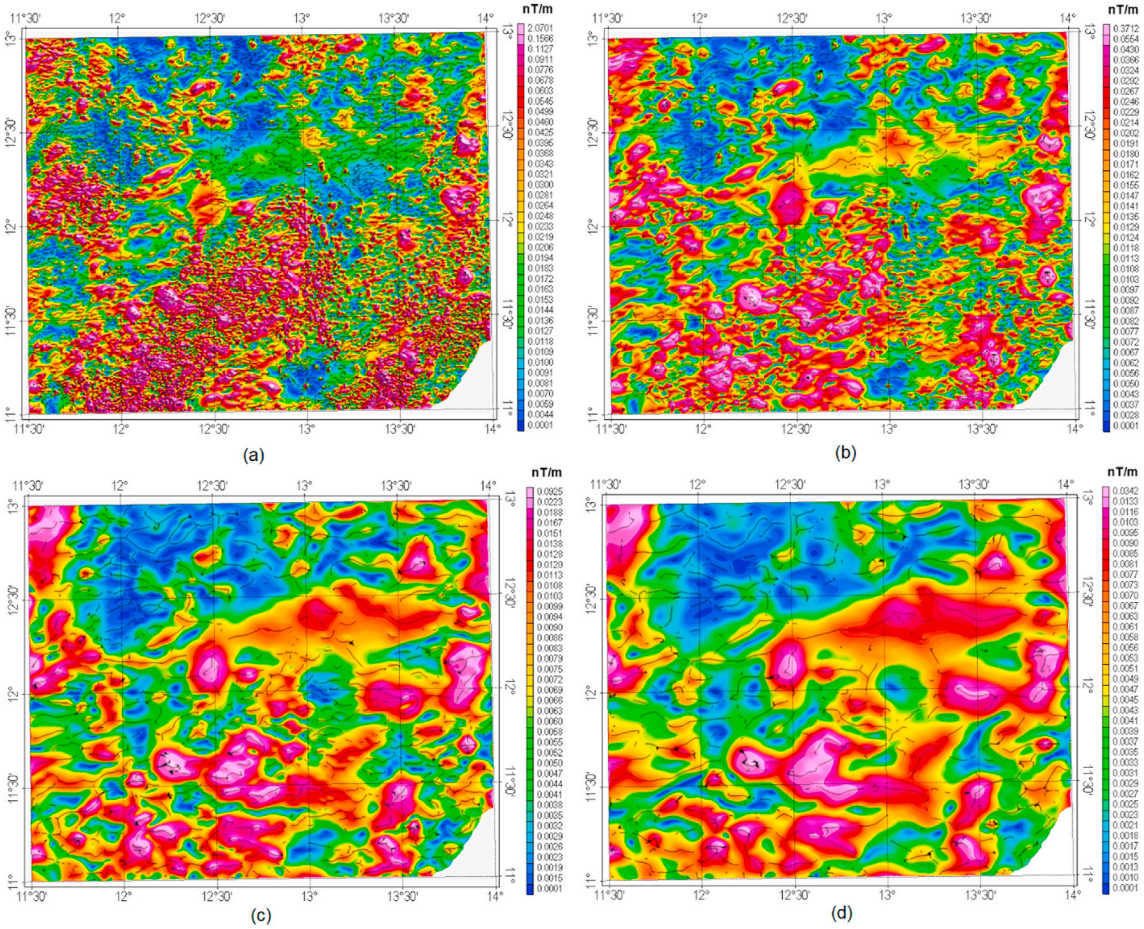

Fig. 8. Analytic Signal maps of the RTE anomaly data upward continued to (a) 100 m (b) 1 km (c) 3 km and (d) 5 km. The black lines on the map indicate the lines of the Analytic Signal maxima.

depths of the underlying rocks. Visual inspection of the map revealed that the magnetic anomalies dominantly have E-W, ENE-WSW and NE-SW orientations. Qualitative interpretation suggests that the short wavelength anomalies that are notable in the southern portion of the map are due to the presence of shallow magnetic sources, while the long wavelength and high magnitude magnetic anomaly extending from the lower part of the north-eastern portion towards the central portion corresponds to deep-seated magnetic sources.

The average CPD computed from the magnetic anomalies over the entire study area using the modified centroid method (Fig. 4b) is 16 km. This implies that the average geothermal gradient and heat flow in the area is about 35°C/km and 87 mW/m^2 respectively. The CPD values

(Fig. 6b) obtained from the 12 overlapping blocks (Fig. 5) were gridded (interpolated and extrapolated) over the bounds of the study area to produce the CPD map in Fig. 9a. Fig. 9b shows the heat flow map generated from the gridded CPD values using Equation (4). The contour lines on the heat flow map indicate the estimated geothermal gradients. As shown in Fig. 9a, the CPDs in the study area range from 11 to 19 km. The deepest CPD occur at Monguno and Marte areas in the northeastern part, while the shallowest CPD occur around Gumsa, Wariri and Chungul Buturi in the northwestern part. Previous studies (e.g. Lawal and Nwankwo, 2017) showed that the deepest CPD in the basin is located around Marte area, while Chungul Buturi and its environs are relatively shallow CPD regions of the basin. The geothermal gradients in the study area range between 30 and 49°C/km, while the heat flow range from 75 to 125 mW/m^2. The heat flow values represent the background (or regional) heat flow in the area. The deviation of the BHT thermal gradient values from the estimated background values, as observed in Fig. 7b, might be due to reasons including the existence of secondary heat sources (intrusive/radiogenic) or sinks in the vicinity of the wells.

The analytic signal maps from which lineaments were extracted using curvature analysis are shown in Fig. 8. The Analytic Signal peaks over magnetic source edges, which are interpreted as geological structures. The composite map in Fig. 10 presents the distribution and networks of geological structures in the study area. The lineaments in green, red, blue and black on the map indicate structures that were mapped at upward continuation heights of 100 m, 1 km, 3 km and 5 km respectively. The composite map reveals that the Chad Basin is affected by many structures at different depths. The map also shows geological structures that are limited to shallow depths from those that extend to deep depths or are deep-seated. The extension of a geological structure from shallow depth (green) to deep depth (black) is indicated by the continued presence of lineaments at increasing altitudes of upward continuation. The progressive shifts of lineaments from shallow to deep zones indicate the direction of the down-dip (Awoyemi et al., 2017). Some notable down-dip directions on the map are indicated by yellow arrowheads. The lineaments in green that show no extension downward are shallow-seated and are most likely indicative of intra-sedimentary structural features in the basin. Isolated lineaments in red might be intra-sedimentary contacts/fractures that have no direct relationship with the basement. Lineaments in red that show continuity downward are more likely intra-sedimentary faults that resulted from basement fault propagation. Basement fault propagation in some parts of the Chad Basin was reported by Awoyemi et al. (2016). The lineaments in blue are possibly deep intra-sedimentary structures or structures existing on/near the basement surface. The lineaments in black are deep-seated and are most likely associated with the basement. The lineaments that feature across all levels (i.e. from black to green) on the map are the major structural features in the study area. The existence of many elongated and interconnected structures in the area suggests the likelihood of structural traps and conduits for the flow of hydrocarbon and hydrothermal fluids in the area.

The lineaments in the study area predominantly trend in the E-W direction, followed by the ENE-WSW direction. Other prominent structural trends in the area include the NE-SW and WNW-ESE. The NW-SE trending structures are more notable among the deep-seated lineaments (blue and black). The identified trends are in agreement with the previous works in the Chad Basin (e.g. Aderoju et al., 2016; Awoyemi et al., 2016). The E-W trend is one of the prominent trends in the geology of Nigeria. It is part of the dominant structural grain produced by the reactivation of the Late Precambrian to Cambrian basement terrain zone of weakness by the Pan-African Orogeny (Nwajide, 2013). There are also suggestions that the E-W trend represents the pre-Pan-African fault system (e.g. Emujakporue et al., 2018; Auduson and Onuoha, 2020). The NE-SW and NW-SE trends are the major structural pattern that the Nigerian Chad Basin share with the rest of the Mega Chad Basin. The NE-SW trending structures were produced during the Pan-African crustal consolidation (Okosun, 1995). The NE-SW and ENE-WSW trends have been linked to the precursor rift directions formed during the African Consolidation Stage (Nwajide, 2013; Genik, 1992). The lineament labelled "RS" indicate a regional-scale structure cutting through the entire study area from Damaturu area to Monguno area. Another notable feature on the map is the point labelled "P" at the Gajiram area, which indicates the intersection point of a possible intra-sedimentary conjugate fault system in the basin. The known oil wells in the basin are located exactly on or near the identified geological structural lines in the study area.

Fig. 11 shows the depths to the magnetic sources in the basin. The depths were computed relative to the ground surface. In the absence of intra-sedimentary intrusives, the depths represent sedimentary thicknesses. The source depth map shows the presence of magnetic sources at depths ranging from shallow (<120 m) to deep (>5 km) zones. Several shallow-seated sources were observed around Bama, Maiduguri, Gujeri, Benisheikh and Chungul Bulturi areas. This suggests the presence of intra-sedimentary intrusive bodies in the areas. The blue region labelled SB contains the largest piles of sediments in the basin. This might be a depocenter or large sub-basin in the Chad Basin.

4.1. Implications for geothermal energy in the study area

Geothermal energy-rich zones, which are the primary target in geothermal exploration, are characterized by high geothermal gradient and high heat flow. The result of this study shows that the heat flow values in the study area range from 75 to 125 mW/m^2. This implies that the magnitude of heat flow in the study area is above the global average,

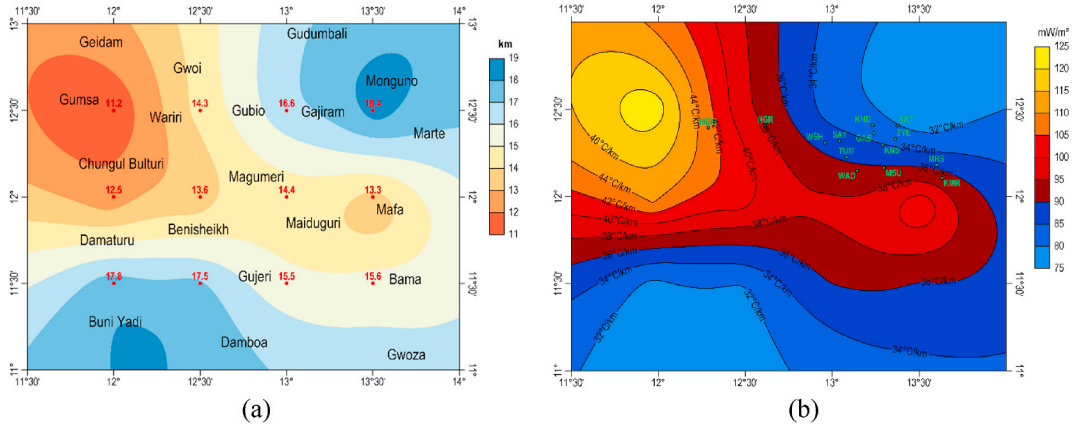

Fig. 9. (a) CPD map showing the DBMS of the study area below the ground surface. (b) Inferred heat flow map of the study area. The contour lines on the heat flow map indicate the estimated geothermal gradients of the study area.

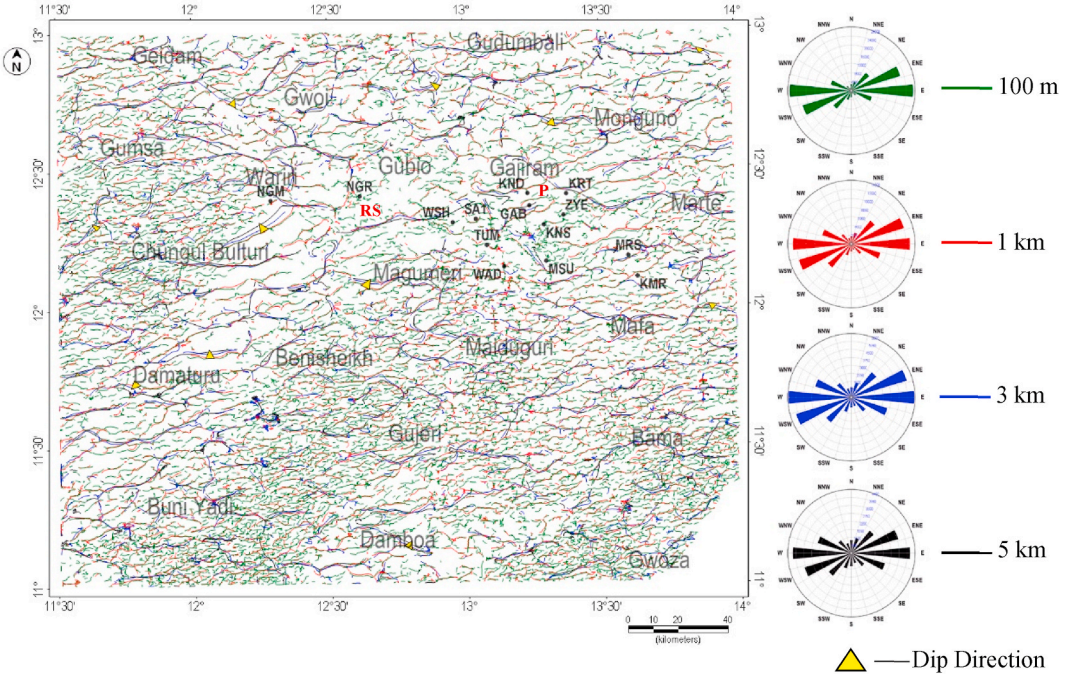

Fig. 10. Composite map of inferred geological structures at different upward continuation heights.

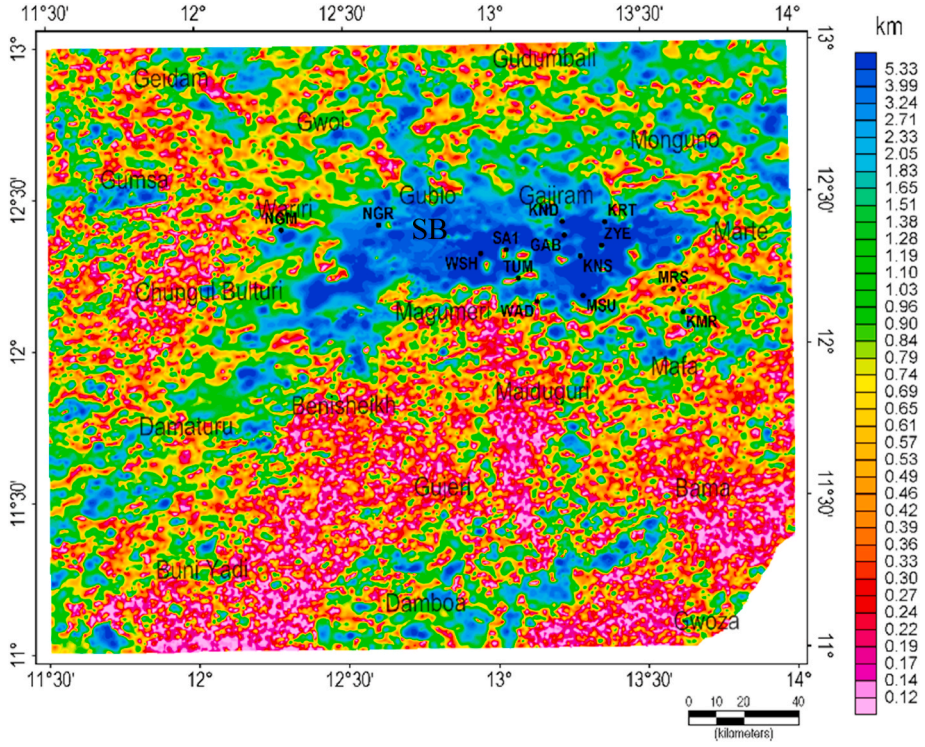

Fig. 11. SPI map showing the depths to magnetic sources in the study area.

which is 65 mW/m^2 in continental crust (Pollack et al., 1993). The heat flow in areas such as Maiduguri, Magumeri and Benisheikh is moderately high (90–100 mW/m^2), while the geothermal condition around Chungul Buturi and Gumsa areas is anomalously high (>100 mW/ m^2). According to Kappelmeyer et al. (1979), the areas having heat flow values that are > 100 mW/m^2 are suitable for the economic exploitation of geothermal energy. This implies that Chungul Buturi and Gumsa are promising areas containing sufficient geothermal energy.

Geothermal exploration involves not only identifying high heat flow regions but also low density, cost-effective regions to drill and major geological structures such as fault or fracture networks within the subsurface that probably control the flow of geothermal fluid. Geological lineaments such as fault lines delineated in geothermal rich zones are good indicators for geothermal exploration targets (Peng et al., 2019). Fault and fracture zones are often identified as prime drilling locations because they are weakness zones with densities much less than the

surrounding rocks; and in addition, faults and fractures serve as hosts for hydrothermal fluids or conduits for their movement. The identified geological structures (Fig. 10) that are elongated and show both shallow (green or red) and deep (black or blue) expressions at or in between Chungul Buturi and Gumsa areas are major geological structures that are more likely to contain valuable geothermal resources that can be exploited easily by drilling.

Apart from the transfer of energy from the crystalline basement into the overlying sedimentary column, intrusive rocks play critical roles in the distribution of geothermal energy in their regions of occurrence within the sedimentary basin. They have enhanced heat production from radioactive decay (Wright et al., 1985) which further reinforces the background geothermal energy. Due to their elevated heat production, they act as reservoirs (collection of hot rocks) from which heat can be drawn. The results obtained in this study (Figs. 10 and 11) show zones of concentrated shallow seated magnetic structures (at depths $<$ 0.5 km), which are believed to be intra-sedimentary intrusive bodies, in Bama, Maiduguri, Benisheikh, Gujeri and Chungul Buturi areas. These intrusive dominated zones may be considered for geothermal resource harnessing in addition to the suggested geothermal rich zones of the Basin.

4.2. Implications for hydrocarbon maturity in the study area

The maturation of hydrocarbon in source rocks is driven by a number of factors. These include the type and organic content (kerogens) of the source rock; duration of sedimentation process; history of sedimentation and burial (depth); and temperature gradient (Palumbo et al., 1999). Information gathered from the literature has shown that the Chad Basin in Nigeria possesses some of these critical criteria, as well as other factors that are essential for high petroleum prospect. These include the age of the basin (Burke, 1969), geochemistry of source rock (Petters and Ekweozor, 1982), sedimentary sequence (Reyment, 1965; Matheis and Kogbe, 1976; Petters, 1981; Okosun, 1995), potential traps (Agagu and Ekweozor, 1980; Avbovbo et al., 1986), and reservoir rocks (Avbovbo et al., 1986; Okosun, 1995). This information is insufficient to ascertain the presence of oil and gas in the basin, as other information about the heat flow variation and sedimentary thickness is needed to gain insights into the rate and extent of maturation of hydrocarbon in the basin. The results of this study provide useful information for assessing the hydrocarbon maturity in the basin. The SPI map (Fig. 11) represents the sedimentary thickness map (in the absence of intra-sedimentary intrusive), while the heat flow map (Fig. 9b) gives insight into the regional heat flow in various parts of the study area. High sedimentary thickness is generally favourable for hydrocarbon maturation and it is one of the key factors that determine the existence of oil and gas windows. Generally, oil window occurs at depths between 2500 ft (~760 m) and 16,000 ft (~4880 m) and natural gas is formed below it (Congress Office of Te, 1989). The SPI map shows sedimentary thicknesses as high as 5 km, and even more, in many parts of the study area (e.g. the southern parts of Gubio and Gajiram). This implies that the existence of oil window within the basin is possible.

Another key factor that determines the maturation of hydrocarbon is geothermal energy. Geothermal energy plays important role in the formation of fluid hydrocarbon. The hydrocarbon maturation of potential source rocks involves a slow cooking (i.e. thermodynamic conversion) of kerogens into fluid hydrocarbon (oil and gas), which then preferentially flow into porous reservoir rocks (Palumbo et al., 1999). The maturation process is highly controlled by the large quantity of heat transferred from the basement into the overlying sedimentary column. This heat controls the phase changes that may take place in the subsurface during the process of hydrocarbon generation, migration and entrapment. However, a negative influence of heat flow may arise when the geothermal energy released to the source rock exceeds their geothermal temperature window. Consequently, the source rocks will become over matured and their kerogen content will be destroyed, which will invariably affect the quantity of hydrocarbon being generated. Also, when the temperature in an oil reservoir exceeds the boiling point of oil but still falls within the temperature window of gas, a phase transition from liquid state (oil) to gaseous state (gas) occurs. However, when the reservoir temperature is too high as a result of high geothermal heat flow through the reservoir, the trapped oil may be boiled off completely over a period of time, giving rise to a dry well. According to Selley (1998), significant crude oil generation occurs at temperatures between $60^{\circ}C$ and $120^{\circ}C$, and considerable gas generation occurs at temperatures between $120^{\circ}C$ and $225^{\circ}C$. The average geothermal gradient of the study area is $35^{\circ}C/km$. With this average, the depth range corresponding to the oil window is 1.7 – 3.4 km. This implies that the basin is thermally matured for the generation of oil, with the possibility of gas being formed beneath it. However, the high magnitudes of background heat flow observed in the study area and the existence of a large number of intrusive bodies in many parts of the basin might have led to the occurrence of overheating during and after fluid hydrocarbon generation and entrapment in many parts of the basin. The exposure of source rocks to excessive heat flow for millions of years could have led to rapid generation of hydrocarbon and evaporation of the accumulated hydrocarbon from the basin. This could have been the reason why the NNPC and other oil firms have been unsuccessful in their search for commercial hydrocarbon accumulation in the area. The oil wells drilled in the basin were mostly dry, while a few had insignificant oil or gas shows (Aderoju et al., 2016). The oil well (Ngammaeast-1) drilled near the anomalous geothermal environment identified in this study was completely dry (Aderoju et al., 2016). The presence of many intrusive bodies in a high geothermal energy environment also suggests that the basin has a higher potential for gas accumulation than oil as reported in earlier studies (Obaje et al., 2004; Petters and Ekweozor, 1982; Olugbemiro et al., 1997). The wells that have gas show in the basin include Kinassar-1, SA-01, Ziye-1, Murshe-01, Krumta-1, and Wadi-01 (Aderoju et al., 2016). The Kanadi-01, Masu-01 and Tuma-01 wells, which have oil show (Aderoju et al., 2016), gives hope on the possibility of finding oil in commercial quantity in the basin.

Future exploration in the Nigerian Chad Basin may be successful if the exploration sites are narrowed down to the areas where the heat flow is moderate for hydrocarbon maturation and thick sedimentary fill with few plutonic rocks were mapped. The region labelled “SB” in Fig. 11 is promising, as it contains high sedimentary thicknesses (about 5 km), moderately high heat flow ($<$100 mWm^{-2}), few shallow seated magnetic bodies (i.e. intrusive), and some elongated geological structures. However, the well locations in Fig. 10 show that many wells have been drilled in the region without success. This might be due to the fact that most intra-sedimentary structures that were targeted in the region, as shown in Fig. 10, were not elongated, and some of the wells (e.g. SA-1 and Tuma-01) were sited at intra-sedimentary intrusive locations. The elongated structure, labelled “RS” (Fig. 10), in the identified promising region is suggested for further investigation in the Nigerian sector of Chad Basin.

5. Conclusion

The geothermal and hydrocarbon potentiality of the selected part of Chad Basin has been determined from the geological structures, depths to magnetic sources and thermal structures inferred from the magnetic anomalies over the area. The Chungul Buturi and Gumsa areas of the basin are promising for economic exploitation of geothermal energy. Some zones containing a large number of shallow-seated magnetic sources in Bama, Maiduguri, Benisheikh, Gujeri and Chungul Buturi are suggested to be intrusive dominated zones that may also contain valuable geothermal resources. The results obtained from this study shows that there is possibility of oil window and the existence of geological structures that could act as conduits and structural traps for the flow of hydrocarbon in the basin. However, the identified geothermal rich zones in the basin might not be favourable for the formation of fluid hydrocarbon. The dry wells encountered in the basin in the past could have

been the consequence of source rocks exposure to excessive heat flow. The most favourable areas for hydrocarbon accumulation in the study area are the regions where moderate heat flow, high sedimentary thicknesses with few shallow seated magnetic sources (intrusives) and elongated geological structures were mapped.

Credit author statement

Musa O. Awoyemi: Supervision, Conceptualization, Methodology, Validation, Writing – review & editing, Sesan C. Falade: Conceptualization, Methodology, Resources, Investigation, Formal analysis, Writing – original draft, Writing – review & editing, Augustine B. Arogundade: Resources, Methodology, Writing – review & editing, Olaide S. Hammed: Methodology, Writing – review & editing, Ojudoo D. Ajama: Methodology, Writing – review & editing, Ayomiposi H. Falade: Resources, Writing – review & editing, Leke S. Adebiyi: Writing – review & editing, Kehinde O. Dopamu: Writing – review & editing, Esther A. Alejolowo: Writing – review & editing.

Declaration of competing interest

The authors declare that they have no known competing financial interests or personal relationships that could have appeared to influence the work reported in this paper.

References

Adegoke, A.K., Sarki Yandoka, B.M., Abdullah, W.H., Akaegbobi, I.M., 2015. Molecular geochemical evaluation of Late Cretaceous sediments from Chad (Bornu) Basin, NE Nigeria: implications for paleodepositional conditions, source input and thermal maturation. Arabian J. Geosci. 8, 1591–1609.

Adekoya, J.A., Ola, P.S., Olabode, S.O., 2014. Possible Bornu Basin hydrocarbon habitat—a review. Int. J. Geosci. 5, 983–996. https://doi.org/10.4236/ijg.2014.59084.

Aderoju, A.B., Ojo, S.B., Adepelumi, A.A., Edino, F., 2016. A reassessment of hydrocarbon prospectivity of the Chad basin, Nigeria, using magnetic hydrocarbon indicators from highresolution aeromagnetic imaging. IFE J. Sci. 18, 503–520.

Agagu, O.K., Ekweozor, C.M., 1980. Petroleum geology of Senonian sediments in Anambra syncline, Southeastern Nigeria: ABSTRACT. Am. Assoc. Petrol. Geol. Bull. 64 https://doi.org/10.1306/2f918a9f-16ce-11d7-8645000102c1865d.

Ahmed, K.S., Liu, K., Moussa, H., Liu, J., Ahmed, H.A., Kra, K.L., 2022. Assessment of petroleum system elements and migration pattern of Borno (Chad) Basin, northeastern Nigeria. J. Petrol. Sci. Eng. 208, 109505.

Auduson, A.E., Onuoha, K.M., 2020. Cretaceous Bida and Sokoto basins of Nigeria: deducing basin architecture and basement topography from aeromagnetic data analyses. Int J Earth Sci Geophys 6, 43.

Avbovbo, A.A., Ayoola, F.O., Osahon, G.A., 1986. Depositional and structural styles in Chad basin of northeastern Nigeria. Am. Assoc. Petrol. Geol. Bull. 70, 1787–1798. https://doi.org/10.1306/94886d21-1704-11d7-8645000102c1865d.

Awoyemi, M.O., Arogundade, A.B., Falade, S.C., Ariyibi, E.A., Hammed, O.S., Alao, O.A., Onyedim, G.C., 2016. Investigation of basement fault propagation in Chad Basin of Nigeria using high resolution aeromagnetic data. Arabian J. Geosci. 9, 453. https://doi.org/10.1007/s12517-016-2465-z.

Awoyemi, M.O., Hammed, O.S., Falade, S.C., Arogundade, A.B., Olayode, F.A., Olurin, O. T., Ajama, O.D., Onyedim, G.C., 2017. Evidence of basement controlled faulting of cretaceous strata in the Middle Benue Trough, Nigeria from lineament analysis of gravity data. IFE J. Sci. 19, 69. https://doi.org/10.4314/ijs.v19i1.8.

Bansal, A.R., Gabriel, G., Dimri, V.P., Krawczyk, C.M., 2011. Estimation of depth to the bottom of magnetic sources by a modified centroid method for fractal distribution of sources: an application to aeromagnetic data in Germany. Geophysics 76, L11–L22. https://doi.org/10.1190/1.3560017.

Bansal, A.R., Anand, S.P., Rajaram, M., Rao, V.K., Dimri, V.P., 2013. Depth to the bottom of magnetic sources (DBMS) from aeromagnetic data of Central India using modified centroid method for fractal distribution of sources. Tectonophysics 603, 155–161. https://doi.org/10.1016/j.tecto.2013.05.024.

Burke, K., 1969. Seismic areas of the Guinea Coast where Atlantic fracture zones reach Africa. Nature 222, 655–657. https://doi.org/10.1038/222655b0.

U.S, 1989. Congress Office of Technology Assessment, Polar Prospects : A Minerals Treaty for Antarctica September 1989. OTA-O-428, Washington D.C.

Dieokuma, T., Sc, M., Ming, G.H., 2013. Preliminary estimation of thermal conductivity in Bornu-Chad basin , Nigeria. Eur. Sci. J. 9, 300–309.

Emujakporue, G., Ofoha, C.C., Kiani, I., 2018. Investigation into the basement morphology and tectonic lineament using aeromagnetic anomalies of Parts of Sokoto Basin, North Western, Nigeria, Egypt. J. Petrol. 27, 671–681.

Frost, B.R., Shive, P.N., 1986. Magnetic mineralogy of the lower continental crust. J. Geophys. Res. 91, 6513. https://doi.org/10.1029/jb091ib06p06513.

Genik, G.J., 1992. Regional framework, structural and petroleum aspects of rift basins in Niger, Chad and the Central African Republic (C.A.R.). Tectonophysics 213, 169–185. https://doi.org/10.1016/0040-1951(92)90257-7.

Kappelmeyer, O., 1979. Implications of heat flow studies for geothermal energy prospects. In: Čermák, V., Rybach, L. (Eds.), Terr. Heat Flow Eur. Springer Berlin Heidelberg, Berlin, Heidelberg, pp. 126–135. https://doi.org/10.1007/978-3-642-95357-6_11.

Kwaya, M.Y., Kurowska, E., Arabi, A.S., 2016. Geothermal gradient and heat flow in the Nigeria sector of the Chad basin, Nigeria, comput. Water, energy. Environ. Eng. 5, 70–78. https://doi.org/10.4236/cweee.2016.52007.

Lawal, T.O., Nwankwo, L.I., 2017. Evaluation of the depth to the bottom of magnetic sources and heat flow from high resolution aeromagnetic (HRAM) data of part of Nigeria sector of Chad Basin. Arabian J. Geosci. 10, 378. https://doi.org/10.1007/s12517-017-3154-2.

Li, C.F., Lu, Y., Wang, J., 2017. A global reference model of Curie-point depths based on EMAG2. Sci. Rep. 7, 45129. https://doi.org/10.1038/srep45129.

MacLeod, I.N., Jones, K., Dai, T.F., 1993. 3-D analytic signal in the interpretation of total magnetic field data at low magnetic latitudes. Explor. Geophys. 24, 679–688. https://doi.org/10.1071/EG993679.

Matheis, G., 1976. Short review of the geology of the Chad basin in Nigeria. In: Kogbe, C. A. (Ed.), Geol. Niger. Elizabethan Publishing, Coy Lagos Nigeria, pp. 289–294.

Mijinyawa, A., Bhattacharya, S.K., Moumouni, A., Mijinyawa, S., Mohammad, I., 2013. Hydrocarbon potentials, thermal and burial history in Herwa-1 well from the Nigerian sector of the Chad basin: an implication of 1-d basin modeling study. Res. J. Appl. Sci. Eng. Technol. 6, 961–968. https://doi.org/10.19026/rjaset.6.3998.

Moumouni, A., 2009. Organic Geochemical, Petrological and Biostratigraphical Evaluations of the Hydrocarbon Prospects of the Nigerian Sector of the Chad Basin. Nigeria.

Nabighian, M.N., Grauch, V.J.S., Hansen, R.O., LaFehr, T.R., Li, Y., Peirce, J.W., Phillips, J.D., Ruder, M.E., 2005. The historical development of the magnetic method in exploration. Geophysics 70, 33ND–61ND. https://doi.org/10.1190/1.2133784.

Nwajide, C.S., 2013. Geology of Nigeria's Sedimentary Basins. CSS Bookshop Limited.

Nwankwo, C.N., Ekine, A.S., 2009. Geothermal gradients in the Chad basin, Nigeria, from bottom Hole temperature logs. Int. J. Phys. Sci. 4, 777–783. https://doi.org/10.5897/IJPS.9000280.

Nwankwo, N.C., Ekine, A.S., Nwosu, L.I., 2009. Estimation of the heat flow variation in the Chad basin Nigeria. J. Appl. Sci. Environ. Manag. 13, 73–80.

Nwankwo, C.N., Emujakporue, G.O., Nwosu, L.I., 2012. Evaluation of the petroleum potentials and prospect of the Chad Basin Nigeria from heat flow and gravity data. J. Pet. Explor. Prod. Technol. 2, 1–6. https://doi.org/10.1007/s13202-011-0015-5.

Obaje, N.G., 2009. Geology and Mineral Resources of Nigeria, 2009th ed. Springer, Berlin, Germany. https://doi.org/10.1007/978-3-540-92685-6.

Obaje, C.E., Abaa, N.G., Najime, S.I., Suh, T., 1999. Economic geology of Nigeria coal resources-a brief review African Geosciences. Afr. Geosci. Rev. 6, 71–81.

Obaje, N.G., Wehner, H., Hamza, H., Scheeder, G., 2004. New geochemical data from the Nigerian sector of the Chad basin: implications on hydrocarbon prospectivity. J. Afr. Earth Sci. 38, 477–487. https://doi.org/10.1016/j.jafrearsci.2004.03.003.

Obaje, N.G., Attah, D.O., Opeloye, S.A., Moumouni, A., 2006. Geochemical evaluation of the hydrocarbon prospects of sedimentary basins in Northern Nigeria. Geochem. J. 40, 227–243. https://doi.org/10.2343/geochemj.40.227.

Okosun, E.A., 1995. Review of the geology of Bornu Basin. J. Min. Geol. 31, 113–122.

Okubo, Y., Matsunaga, T., 1994. Curie point depth in northeast Japan and its correlation with regional thermal structure and seismicity. J. Geophys. Res. 99, 22363–22371. https://doi.org/10.1029/94jb01336.

Okubo, Y., Graf, R.J., Hansen, R.O., Ogawa, K., Tsu, H., 1985. Curie point depths of the Island of Kyushu and surrounding areas, Japan. Geophysics 50, 481–494. https://doi.org/10.1190/1.1441926.

Olugbemiro, R.O., Ligouis, B., Abaa, S.I., 1997. The Cretaceous series in the Chad Basin, NE Nigeria: source rock potential and thermal maturity. J. Petrol. Geol. 20, 51–68. https://doi.org/10.1111/j.1747-5457.1997.tb00755.x.

Palumbo, F., Main, I.G., Zito, G., 1999. The thermal evolution of sedimentary basins and its effect on the maturation of hydrocarbons. Geophys. J. Int. 139, 248–260. https://doi.org/10.1046/j.1365-246X.1999.00877.x.

Peng, C., Pan, B., Xue, L., Liu, H., 2019. Geophysical survey of geothermal energy potential in the Liaoji Belt, northeastern China. Geotherm. Energy. 7, 14. https://doi.org/10.1186/s40517-019-0130-y.

Petters, W., 1981. Stratigraphy of Chad and Iullemmeden basins (west Africa). Eclogae Geol. Helv. 74, 139–159. http://www.e-periodica.ch.

Petters, S.W., Ekweozor, C.M., 1982. Petroleum geology of benue trough and Southeastern Chad basin, Nigeria. AAPG Bull. V 66, 1141–1149. https://doi.org/10.1306/03B5A65B-16D1-11D7-8645000102C1865D.

Phillips, J.D., Hansen, R.O., Blakely, R.J., 2007. The use of curvature in potential-field interpretation. Explor. Geophys. 38, 111–119. https://doi.org/10.1071/EG07014.

Pollack, H.N., Hurter, S.J., Johnson, J.R., 1993. Heat flow from the Earth's interior: analysis of the global data set. Rev. Geophys. 31, 267–280. https://doi.org/10.1029/93RG01249.

Quintero, W., Campos-Enríquez, O., Hernández, O., 2019. Curie point depth, thermal gradient, and heat flow in the Colombian Caribbean (northwestern South America). Geotherm. Energy. 7, 16. https://doi.org/10.1186/s40517-019-0132-9.

Ravat, D., Pignatelli, A., Nicolosi, I., Chiappini, M., 2007. A study of spectral methods of estimating the depth to the bottom of magnetic sources from near-surface magnetic anomaly data. Geophys. J. Int. 169, 421–434. https://doi.org/10.1111/j.1365-246X.2007.03305.x.

Reyment, R.A., 1965. Aspects of the Geology of Nigeria, vol. 145. Univ. Ibadan Press, Ibadan.

Ross, H.E., Blakely, R.J., Zoback, M.D., 2006. Testing the use of aeromagnetic data for the determination of Curie depth in California. Geophysics 71, L51–L59. https://doi.org/10.1190/1.2335572.

Selley, R.C., 1998. Elements of Petroleum Geology, second ed. Academic Press, San Diego, California.

Shirputda, J.J., 2019. Assessment of Geothermal Resources in the Nigerian Sector of the Chad Basin. Ne-Nigeria.

Stacey, F.D., 1977. Physics of the Earth, second ed. John Wiley and Sons, New York.

Tanaka, A., Okubo, Y., Matsubayashi, O., 1999. Curie point depth based on spectrum analysis of the magnetic anomaly data in East and Southeast Asia. Tectonophysics 306, 461–470.

Thurston, J.B., Smith, R.S., 1997. Automatic conversion of magnetic data to depth, dip, and susceptibility contrast using the SPI (TM) method. Geophysics 62, 807–813. https://doi.org/10.1190/1.1444190.

Tyoh, A.A., Uko, E.D., Ayanninuola, O.S., Davies, O.A., 2021. Effects of near-surface air temperature on sub-surface geothermal gradient and heat flow in Bornu-Chad basin, Nigeria. Int. J. Terr. Heat Flow Appl. 4, 95–102. https://doi.org/10.31214/ijthfa.v4i1.68.

Wright, P.M., Ward, S.H., Ross, H.P., West, R.C., 1985. State-of-the-art geophysical exploration for geothermal resources. Geophysics 50, 2666–2699. https://doi.org/10.1190/1.1441889.